Title: Climate variability and flow management impact phytoplankton biomass in a shallow reservoir

Electronic Supplementary Information (ESI)

Comparison of flows from Lake Diefenbaker and Buffalo Pound Lake's catchment

Flow rates differ amongst catchment sources and Lake Diefenbaker. Because BPL is in a dryland region with highly intermittent precipitation, flows into BPL are dominated by releases from Lake Diefenbaker in most years (Figure S1). While flows from Lake Diefenbaker are higher on average in summer compared to other seasons and to flows from the watershed, mean and maximum watershed flows can be greater than or similar to flow rates from Lake Diefenbaker in spring months.

Note that flow from watershed sources (QWS) was reconstructed using non-linear regression (1). Daily average flow from watershed sources included flow from Ridge Creek, a tributary to the Qu'Appelle River, and reconstructed flow from Iskwao Creek, provided by the Saskatchewan Water Security Agency (WSA). Flow from Iskwao Creek was measured until 2007; flow estimates following this year have been reconstructed using non-linear regression (1). The contribution of flow from watershed sources was estimated by adding together the flows from Iskwao and Ridge Creeks and scaling up to the effective watershed area to reflect ungauged portions of the watershed (1). Note that watershed flows are intermittent (highly 0-inflated).

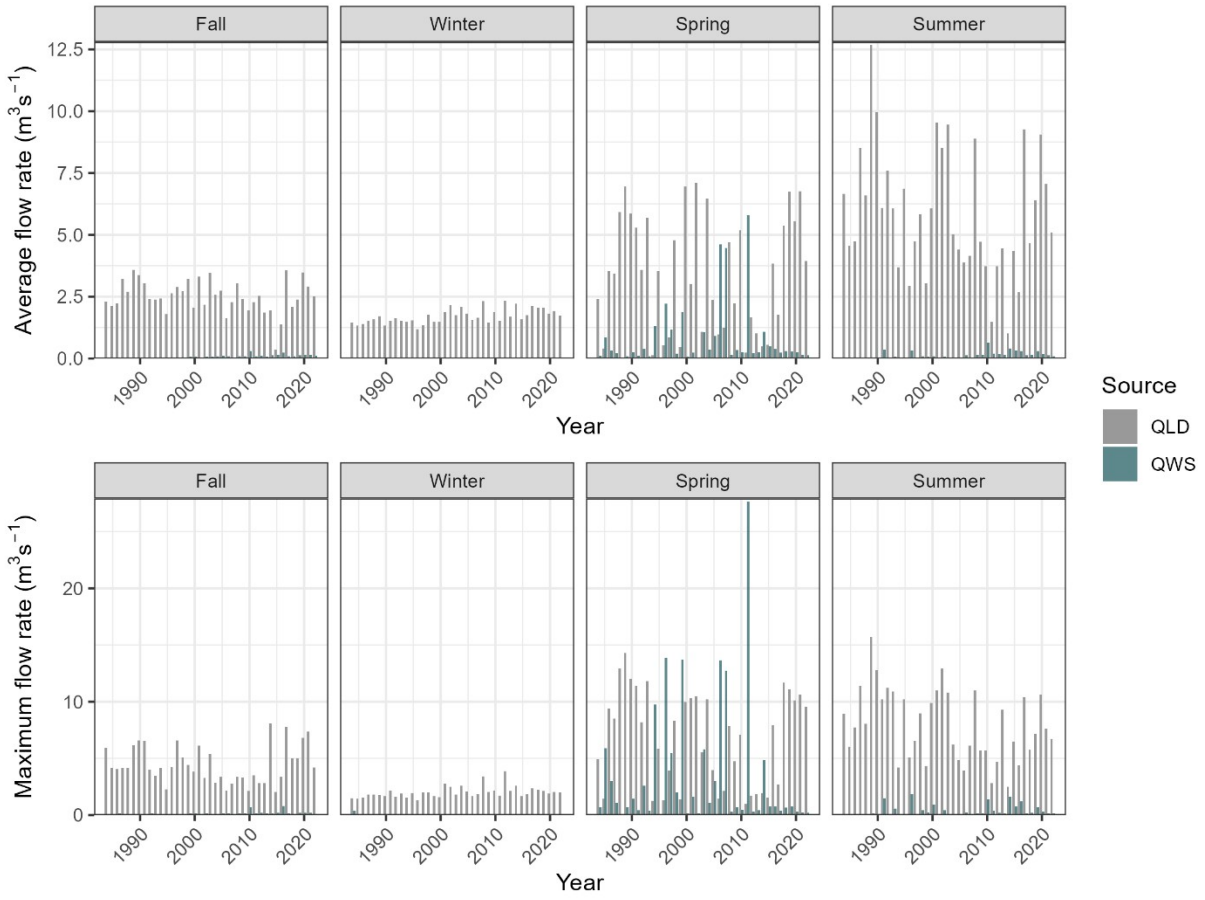

Figure S1: Comparison of average and maximum flow rates across each season and year from different sources to Buffalo Pound Lake, including Lake Diefenbaker and catchment flows. Data represent daily average flows at each sampling site between 1984 and 2022.

Importantly, flows from Lake Diefenbaker are related to flows from the catchment via changes in flow releases from Lake Diefenbaker—releases from Lake Diefenbaker are typically paused or slowed during wet periods with high catchment flows to prevent downstream flooding, and increased during dry periods to maintain water levels in BPL (Figure S2). For example, high flows from the watershed (e.g., above 10 $m^3 s^{-1}$) does not co-occur with high flows from Lake Diefenbaker (e.g., above 5 $m^3 s^{-1}$).

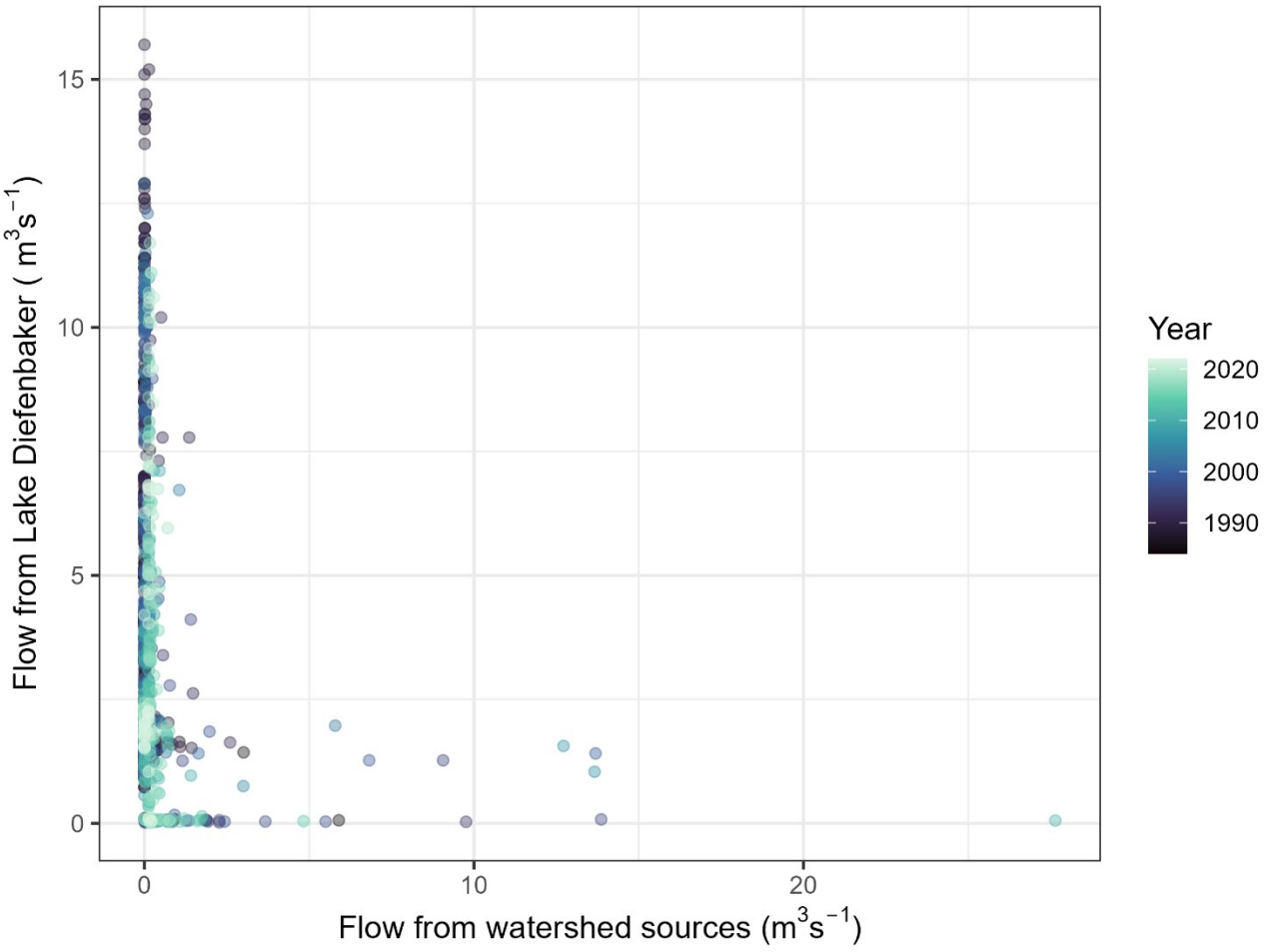

Figure S2: Scatterplot showing flow rates (m^3 s^{-1}) from Lake Diefenbaker and watershed sources across the timeseries. Data are daily average flows from 1984–2022.

The two decades with the highest flows from catchment sources (QWS) were the 1990s (26%) and 2010s (35.5%), followed by the 19.5% in the 2000s (Figure S3). Approximately 8% of all high watershed flow events occurred between 1984 and 1998, and 11% occurred between 2020–2022. High watershed flow events are defined as flow rates that fall within the 75th percentile of all watershed flow data.

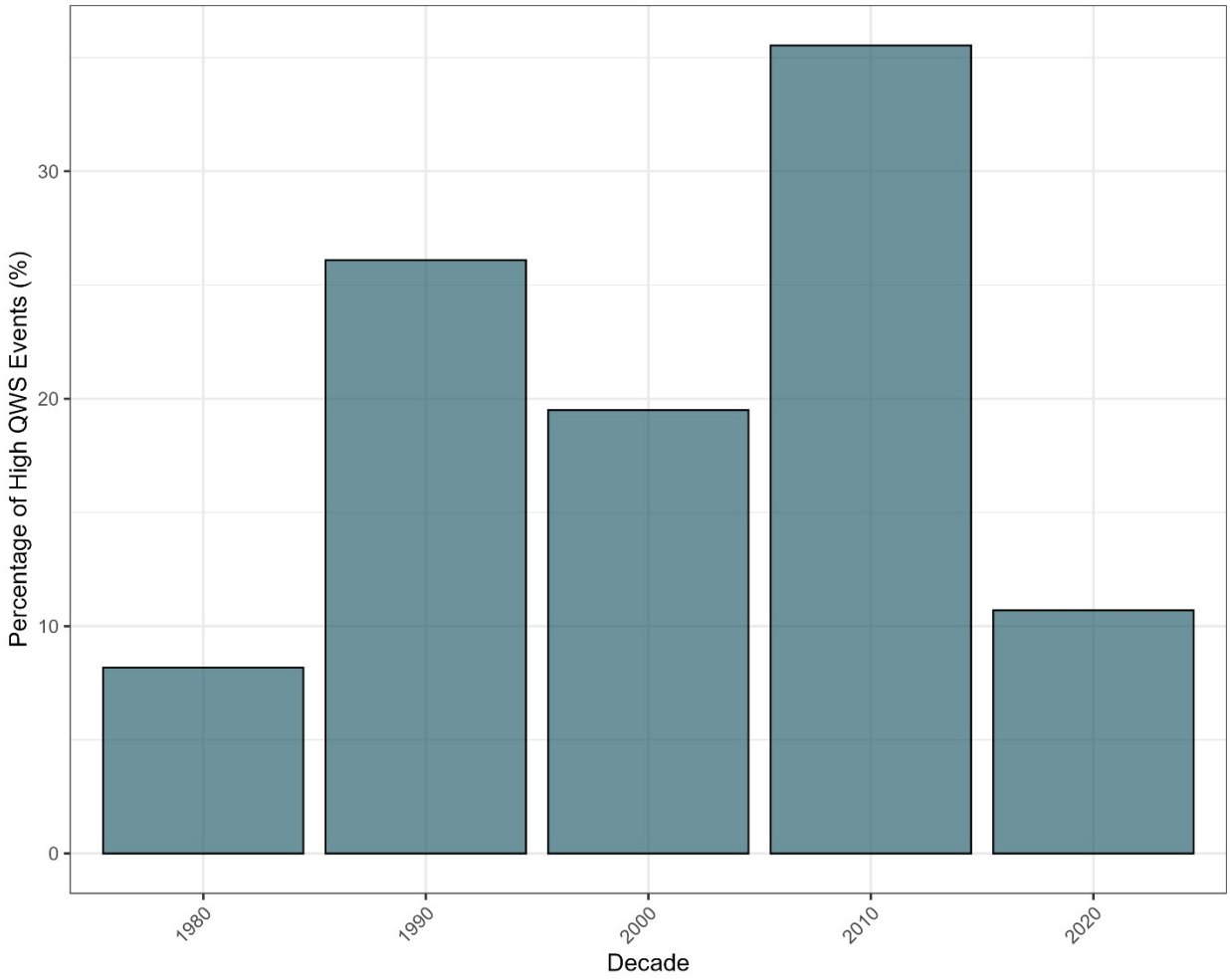

Figure S3: Percentage of high watershed flow (QWS) events that occurred across each decade between 1984 and 2022. High watershed flows are defined here as flows within the 75th percentile of all observations.

Flow sources to Buffalo Pound Lake

Given the distance between flows from Lake Diefenbaker, catchment tributaries, and BPL, as well as the difference in natural catchment boundaries between BPL and Lake Diefenbaker, water chemistry varies amongst these sources and changes as it travels downstream towards BPL (Figure S4). For example, flows from Lake Diefenbaker (here named Highway 19, which is the first sampling location downstream of the Qu'Appelle Dam on Lake Diefenbaker) tend to be mesotrophic (lower in nutrient concentrations) compared to all other sources. In comparison, catchment inflows (Iskwao Creek and Ridge Creek, the two primary local catchment tributaries) tend to have higher nutrient concentrations (ammonia, total nitrogen, total phosphorus, and total reactive phosphorus), except for nitrate and nitrite which have comparable concentrations to outflows from Lake Diefenbaker across the sampling years. Additionally, episodic backflow events from the downstream tributary, the Moose Jaw River (the Buffalo Pound-outflow site), during particularly wet periods contributes greater nutrient loads to Buffalo Pound Lake (2). The Marquis sampling site represents the sampling location immediately upstream of Buffalo Pound Lake, demonstrating that water chemistry changes as it travels downstream from Lake Diefenbaker and catchment tributaries to Buffalo Pound Lake.

Note that all data used in Figure S4 were extracted from the Qu'Appelle nutrient mass balance report 2013-2016 and represent the volume-weighted nutrient concentrations (all in $\mu g\ L^{-1}$) measured at each sampling site between March 1, 2013 and February 29, 2016 (2). Total Reactive Phosphorus (TRP) is a measure of the reactive phosphorus available in a water sample, primarily in the form of orthophosphate ions but may also include other soluble organic phosphorus compounds.

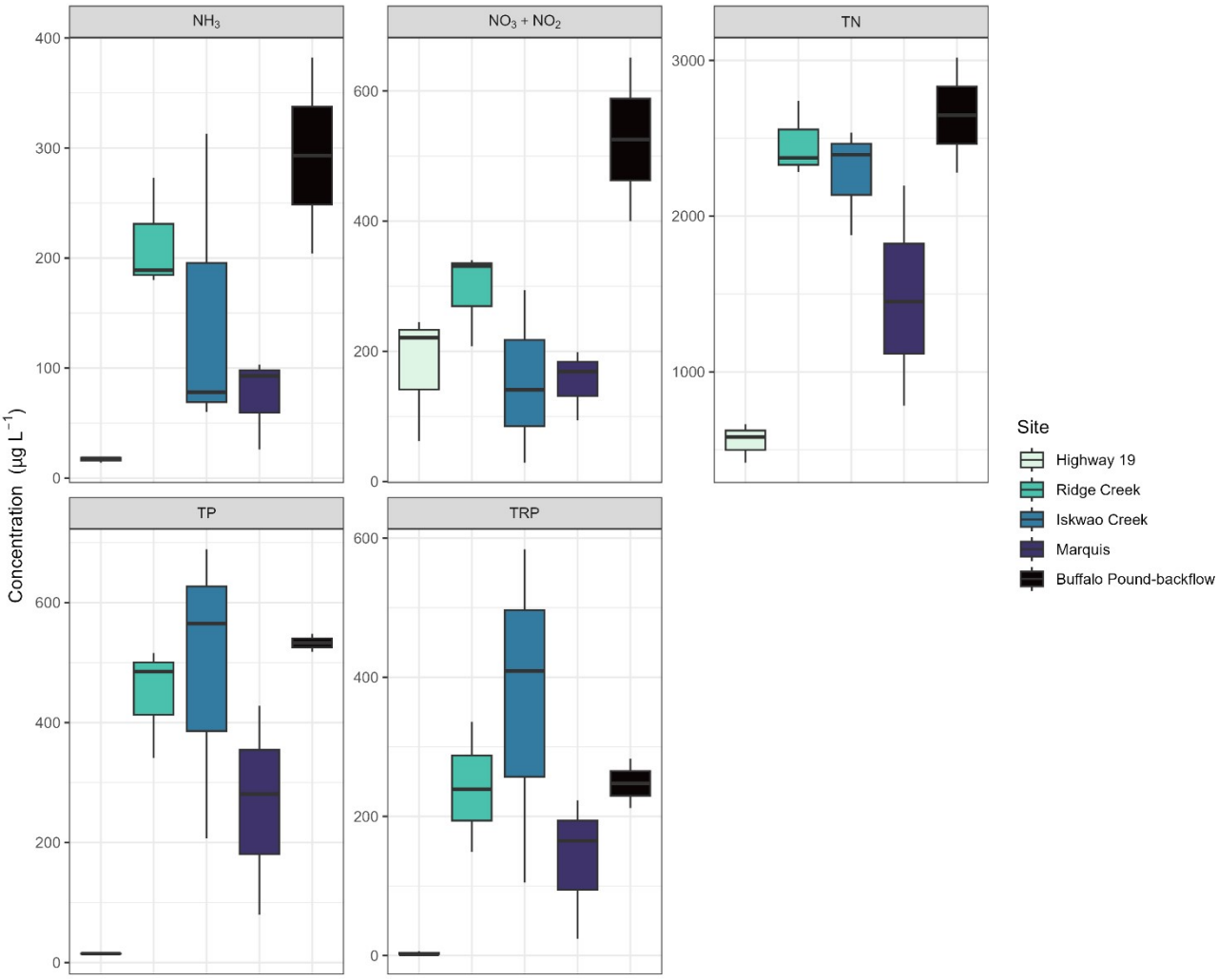

Figure S4: Comparison of water chemistry across primary flow sources to Buffalo Pound Lake, including Lake Diefenbaker (Highway 19 site), catchment inflows (Ridge Creek and Iskwao Creek), immediately upstream of Buffalo Pound Lake, and episodic backflow events from the downstream tributary (Buffalo Pound-backflow). Sites are organized by approximate position along the Qu'Appelle River, starting with sites upstream of Buffalo Pound Lake (Lake Diefenbaker and the two local catchment tributaries, Ridge Creek and Iskwao Creek) and moving downstream, concluding at the backflow site at the downstream tributary. Data represent the volume-weighted nutrient concentrations (all in µg L^{-1}) measured at each sampling site between March 1, 2013 and February 29, 2016 (2). Parameters include ammonia (and ammonium, here described as NH_3), nitrite and nitrate ($NO_3 + NO_2$), total nitrogen (TN), total phosphorus (TP), and total reactive phosphorus (TRP).

SOI and PDO index values

Figure S5 shows annual average SOI and PDO index values. The positive phase of SOI represents cooler, wetter periods on the Canadian Prairies, whereas the negative phase represents warmer, drier periods. In contrast, the negative phase of PDO represents cooler periods, and the positive phase represents warmer periods on the Canadian Prairies.

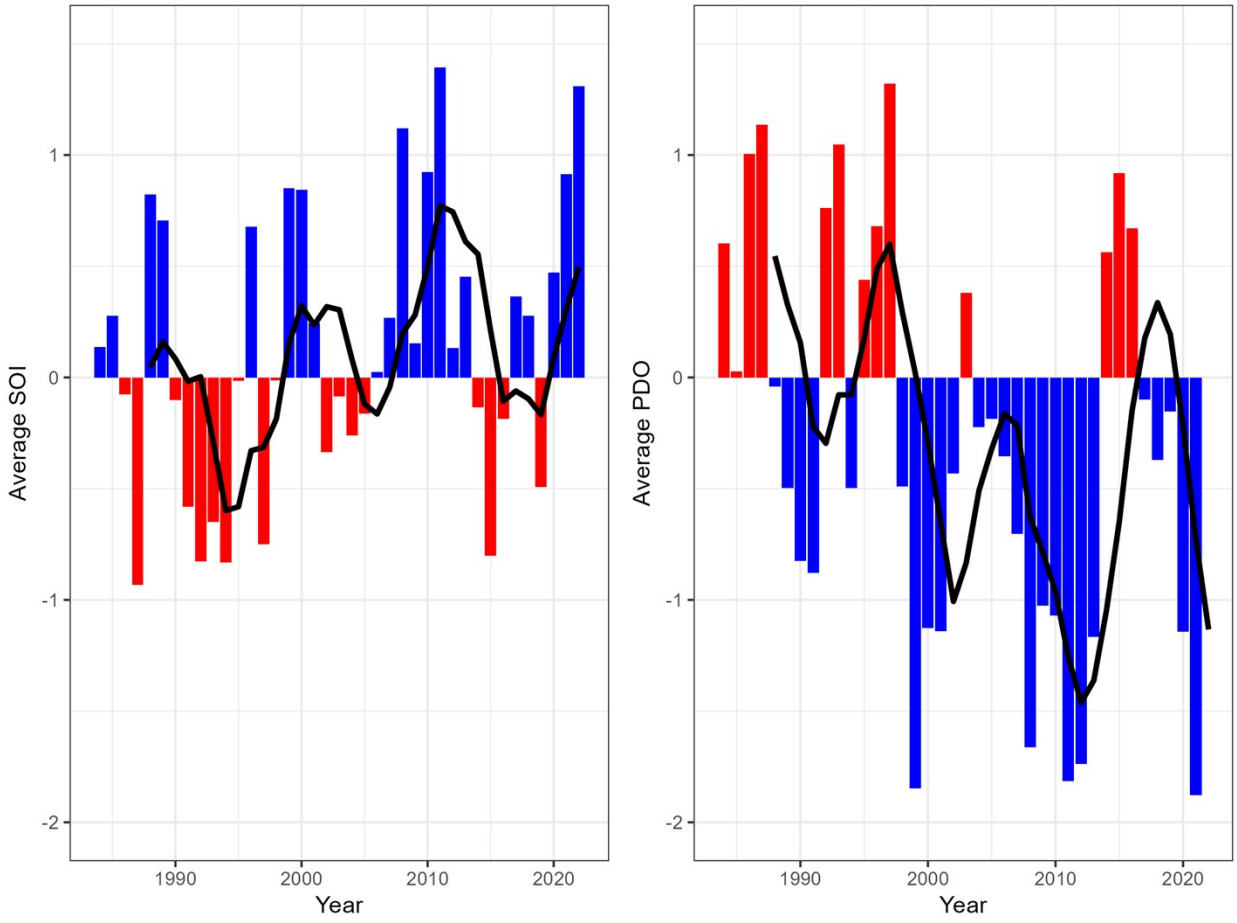

Figure S5: Average annual index values for the Southern Oscillation Index (SOI) and Pacific Decadal Oscillation (PDO) between 1984 and 2022. Black line represents the 5-year moving average, the blue bars represent cold phases, and the red bars represent the warm phases. Data downloaded from the National Centers for Environmental Information's website (3,4).

Models with 6-month lag applied

Comparisons of generalized additive models (GAMs) with and without a 6-month lag applied to the 3-month averages of SOI and PDO index values showed no substantial differences. As with the model without the 6-month lag applied, the model with the 6-month lag applied showed that all included environmental variables were significant predictors of variability in chl.*a* concentrations (Table S1). All predictors had p values < 0.0001 and the model explained 61% of deviance.

Table S1: Summary of additive modelling of the estimated effect of environmental predictors chlorophyll *a* concentrations. Adjusted $R^2 = 0.534$, n = 1084.

Predictor	EDF	DF	p-value
Soluble reactive phosphorus	5.0	9	< 0.0001
Dissolved inorganic nitrogen	6.1	9	< 0.0001
Lake Diefenbaker flow	1.0	6	< 0.0001
te(SOI, PDO)	13.7	24	< 0.0001
te(Year, DOY)	63.9	109	< 0.0001

As with analyses without the 6-month lag applied to the 3-month averages of SOI and PDO index values, models with the 6-month lag applied show that at negative SOI and positive PDO index values (typical of warm, dry conditions, particularly in summer), particularly around index values of -1 to -2 for SOI and between -1 to 1.5 for PDO, GAM-modelled chl.*a* concentrations were higher (Figure S6)..

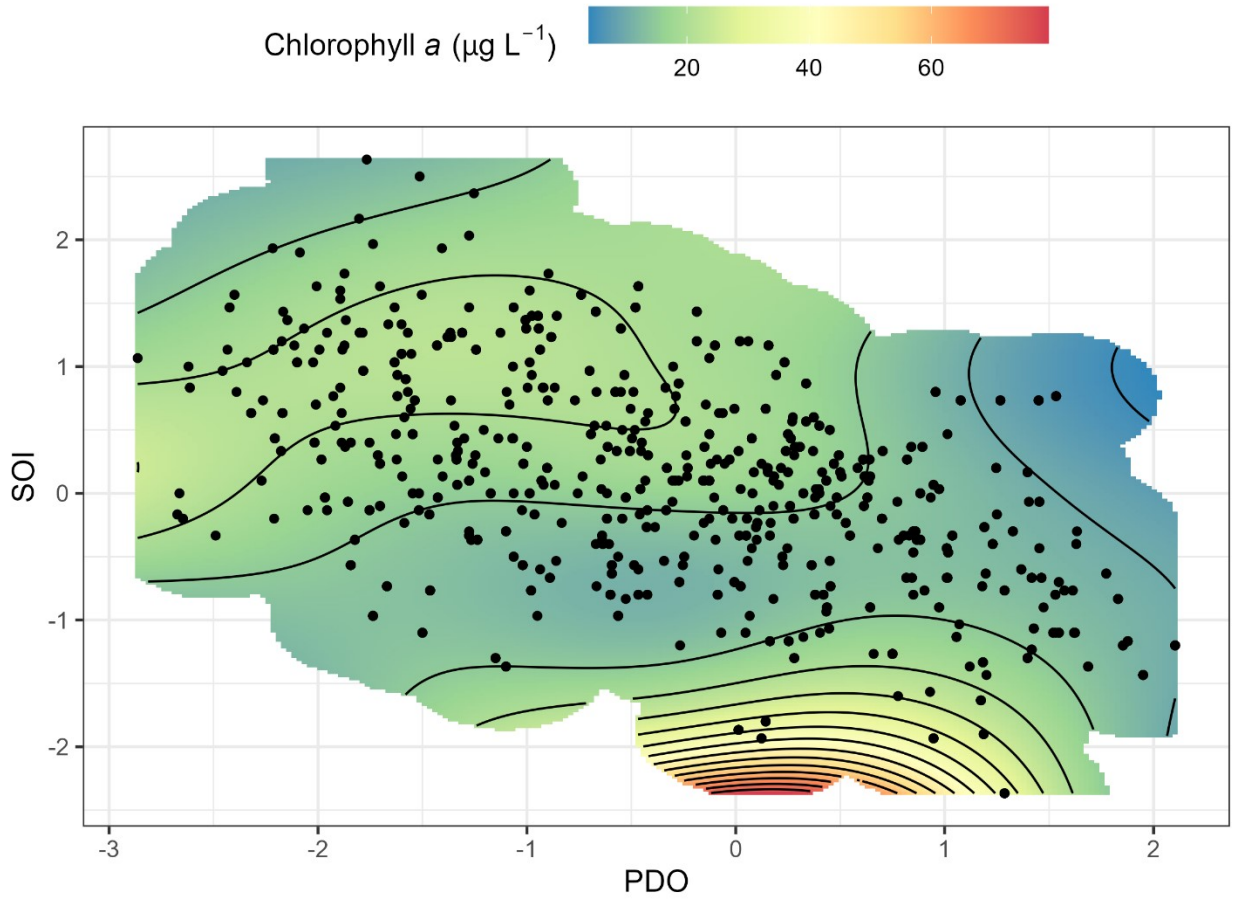

Figure S6: Fitted chlorophyll *a* estimates predicted using additive modelling of a tensor product interaction between the 3-month average of SOI and PDO index values with a 6-month lag applied. Lower ends of the colour spectrum (blues and greens) represent lower modelled chlorophyll *a* concentrations whereas higher ends (yellow, orange, and red) indicate higher modelled chlorophyll *a* concentrations. Interannual variability in relationships (specified as a tensor product of year and DOY) have also been accounted in this model but are not shown here.

Model fit: Time series GAMM

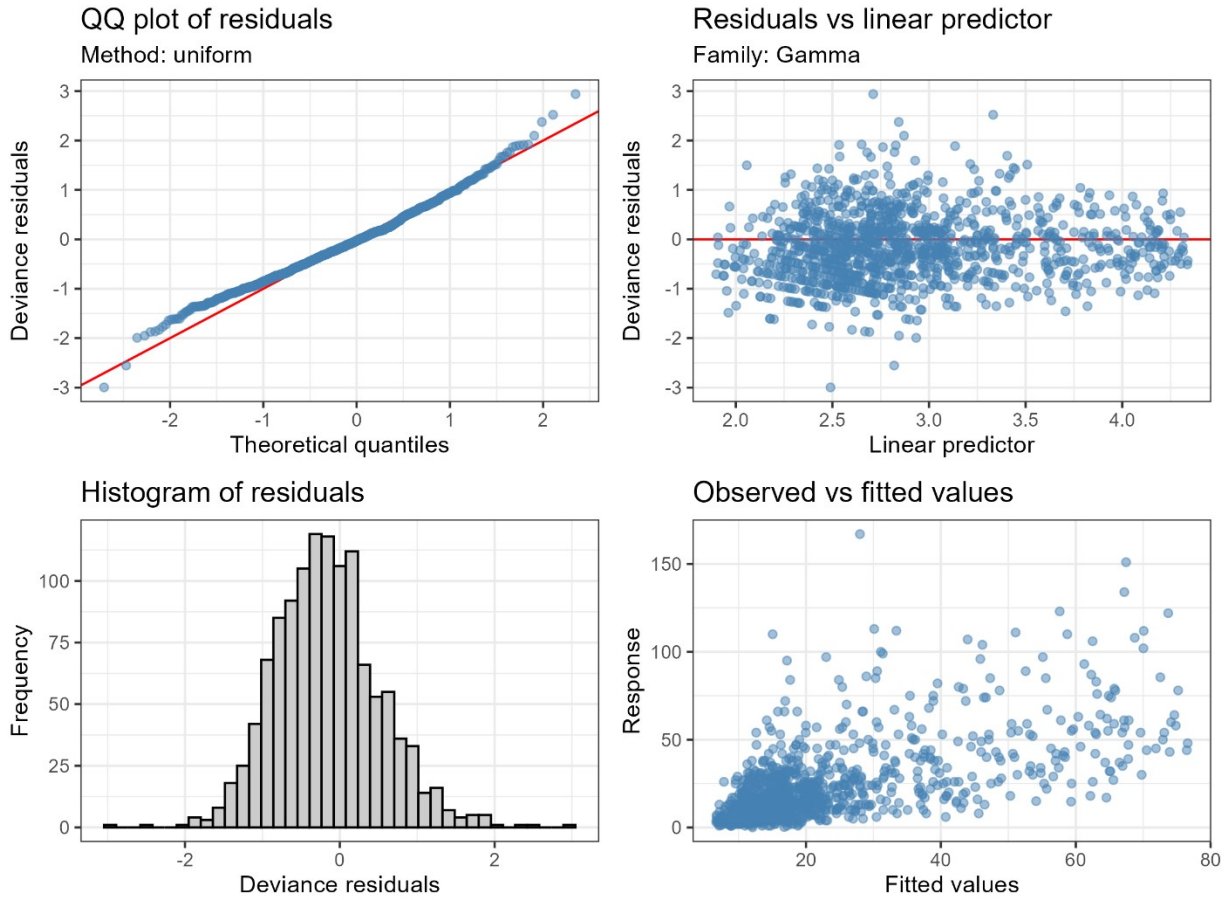

Figure S7: Model diagnostics of generalized additive mixed models used to assess temporal trends in chlorophyll *a*.

Model fit: GAM with predictors

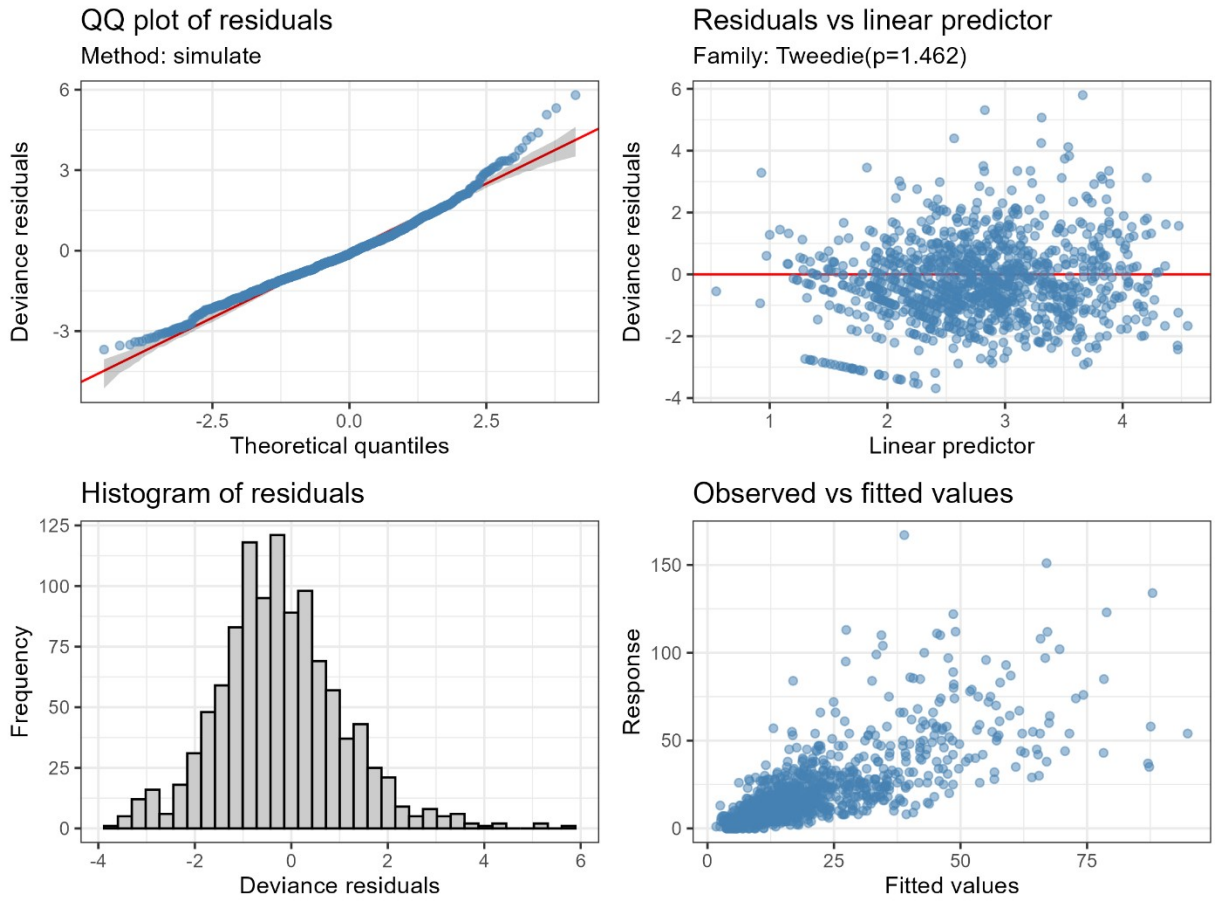

Figure S8: Model diagnostics of generalized additive models used to assess the effects of climate variability, flow source, and nutrients on Chl *a* concentrations.

Timeseries of environmental variables

Figure S9 presents a timeline of key environmental variables over time in BPL, including Chl *a* concentrations and nutrient concentrations (soluble reactive phosphorus or SRP and dissolved inorganic nitrogen or DIN), flow from Lake Diefenbaker (QLD), and flow from watershed sources (QWS). Light pink and blue shaded rectangles indicate periods where ENSO and PDO were in-phase, with pink indicating the warm/dry phase and blue indicating the cool/wet phase. The red box overlain in Figure S9 represents the period of significant increase in Chl *a* concentrations. Importantly, the red box in Figure S9 shows that nutrients (SRP and DIN,), as well as watershed flows (QWS), were relatively high within the period of significant increase in Chl *a* concentrations (especially between 1995–2000), suggesting that watershed flows and nutrients (likely carried into Buffalo Pound Lake via flows from catchment tributaries) potentially contributed to the period of significant increase in phytoplankton biomass. A period of suppressed phytoplankton biomass occurred between ~2007–2010, which corresponded to a period with higher inputs from Lake Diefenbaker (QLD). Additionally, after 2007, annual median, max, and min DIN concentrations decreased, while SRP max, min, and median concentrations decreased after 2005.

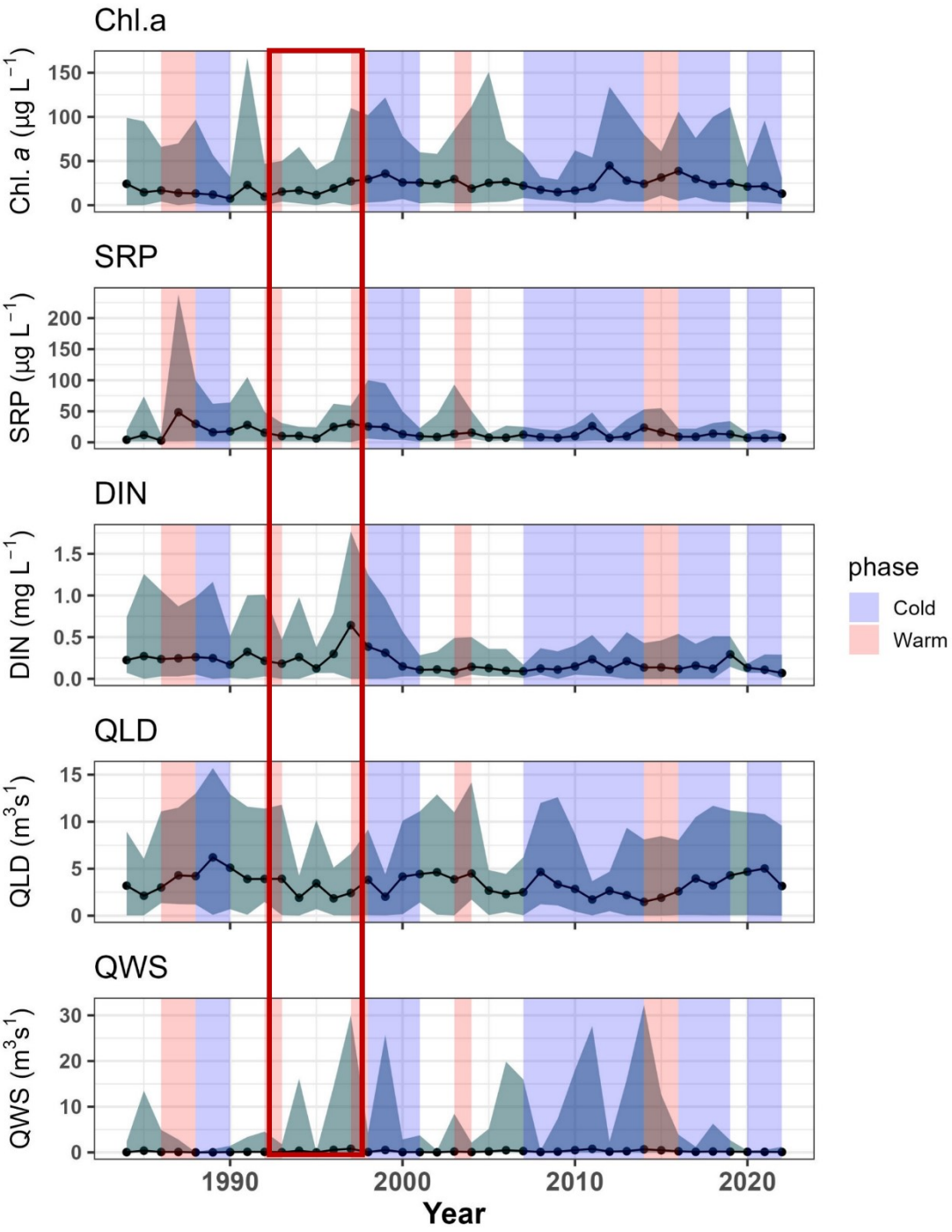

Figure S9: Comparison of annual median values for chlorophyll *a* (Chl *a,* µg/L), soluble reactive phosphorus (SRP, µg/L), and dissolved inorganic nitrogen (DIN, mg/L) in Buffalo Pound Lake, as well as flow from Lake Diefenbaker (QLD, $m^3 s^{-1}$), and flow from the watershed (Iskwao Creek and Ridge Creek, QWS, $m^3 s^{-1}$). Blue-grey ribbons show minimum and maximum values. Red rectangle encases the period of significant change in chlorophyll *a* concentrations (from August 1992– November 1997). Shaded rectangles indicate phases where both ENSO and PDO were in-phase, with light pink rectangles indicating the warm/dry phases of both, and blue rectangles indicating the cool/wet phases of both.

Over the past 39 years, mean and maximum water temperatures in BPL were variable (Figure S10). The warmest average water temperature occurred in 2020 (~11.7 ℃), followed by 1991 (~11.6 ℃). The highest water temperature recorded occurred in August 2022 (27.7 ℃). Water temperatures were measured at the Buffalo Pound Water Treatment Plant between 1984 and 2022.

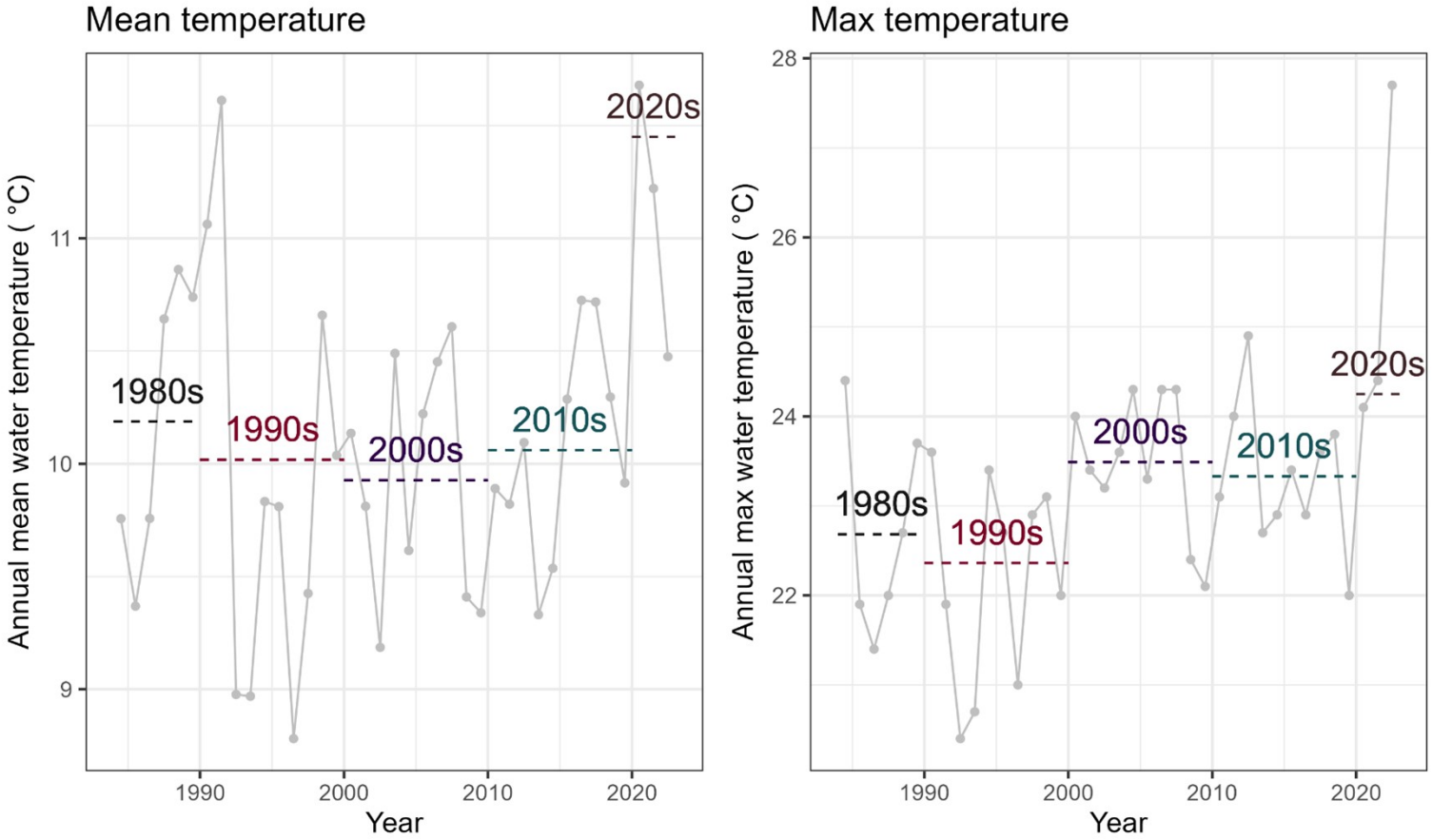

Figure S10: Average annual mean (left) and max (right) water temperatures (˚C) for each year, with averages for each decade between 1984–2022.

Mean summer (June–September) water temperatures show an overall increasing trend across the timeseries, increasing from and average of ~18.2℃ in the 1980s and 1990s to 19℃ in the 2010s (Figure S11). The average summer water temperature in 2020–2022 was highest, reaching above 20℃. Maximum summer water temperatures were more variable, with decadal averages ranging between ~22.2℃ in the 1990s to ~24.1℃ in 2020–2022.

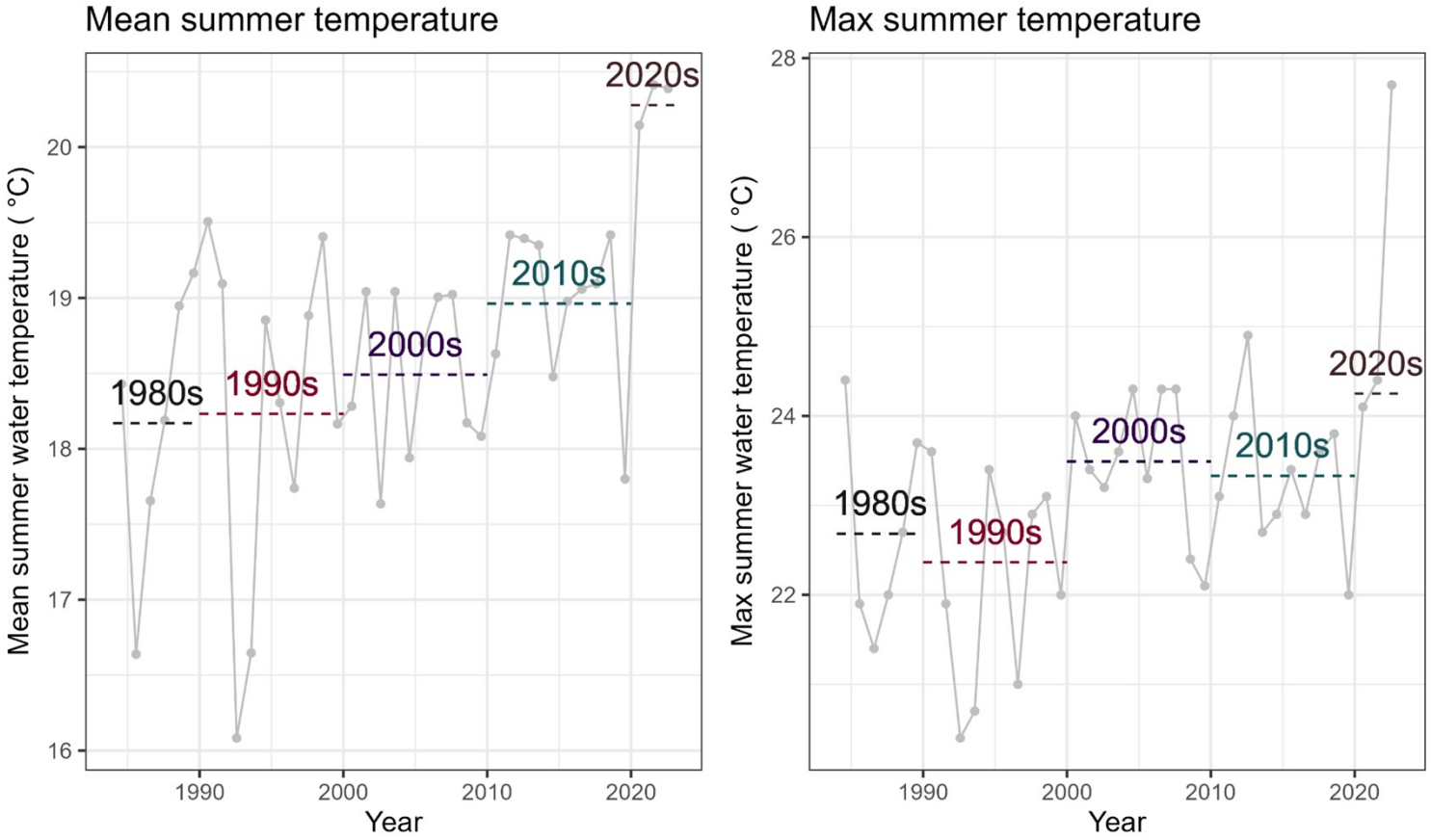

Figure S11: Average summer (June–September) mean (left) and max (right) water temperatures (˚C) for each year, with averages for each decade between 1984–2022.

References

1. Baron AAP, Baulch HM, Nazemi A, Whitfield CJ. Novel statistical analysis illustrates importance of flow source for extreme variation in dissolved organic carbon in a eutrophic reservoir in the Great Plains. Hydrol Earth Syst Sci. 2025;29:1449–68.
2. Vandergucht DM, Perez-Valdivia C, Davies JM. Qu'Appelle nutrient mass balance report 2013-2016 [Internet]. 2018. Available from: https://www.wsask.ca/wp-content/uploads/2021/03/The-QuAppelle-Nutrient-Mass-Balance-Report.pdf
3. NCEI. Pacific Decadal Oscillation [Internet]. 2025. Available from: https://www.ncei.noaa.gov/access/monitoring/pdo/
4. NCEI. El Niño-Southern Oscillation [Internet]. 2025. Available from: https://www.ncei.noaa.gov/access/monitoring/enso/soi